The Power of Sample Multiplexing
With TotalSeq™ Hashtags
Read our app note
BioLegend®

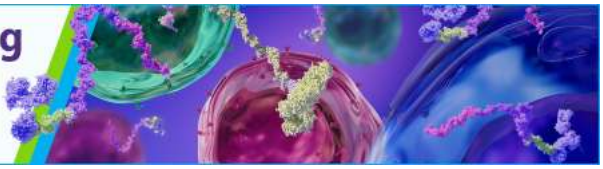

The Journal of Immunology

This information is current as of August 4, 2022.

Tumor-Associated Microglia/Macrophages Enhance the Invasion of Glioma Stem-like Cells via TGF-β1 Signaling Pathway

Xian-zong Ye, Sen-lin Xu, Yan-hong Xin, Shi-cang Yu, Yi-fang Ping, Lu Chen, Hua-liang Xiao, Bin Wang, Liang Yi, Qing-liang Wang, Xue-feng Jiang, Lang Yang, Peng Zhang, Cheng Qian, You-hong Cui, Xia Zhang and Xiu-wu Bian

J Immunol 2012; 189:444-453; Prepublished online 4 June 2012;
doi: 10.4049/jimmunol.1103248
http://www.jimmunol.org/content/189/1/444

Supplementary Material http://www.jimmunol.org/content/suppl/2012/06/04/jimmunol.1103248.DC1

References This article **cites 56 articles**, 6 of which you can access for free at:
http://www.jimmunol.org/content/189/1/444.full#ref-list-1

Why *The JI*? Submit online.

- **Rapid Reviews! 30 days*** from submission to initial decision
- **No Triage!** Every submission reviewed by practicing scientists
- **Fast Publication!** 4 weeks from acceptance to publication

**average*

Subscription Information about subscribing to *The Journal of Immunology* is online at:
http://jimmunol.org/subscription

Permissions Submit copyright permission requests at:
http://www.aai.org/About/Publications/JI/copyright.html

Email Alerts Receive free email-alerts when new articles cite this article. Sign up at:
http://jimmunol.org/alerts

The Journal of Immunology is published twice each month by
The American Association of Immunologists, Inc.,
1451 Rockville Pike, Suite 650, Rockville, MD 20852
Copyright © 2012 by The American Association of Immunologists, Inc. All rights reserved.
Print ISSN: 0022-1767 Online ISSN: 1550-6606.

Downloaded from http://www.jimmunol.org/ by guest on August 4, 2022

Tumor-Associated Microglia/Macrophages Enhance the Invasion of Glioma Stem-like Cells via TGF-β1 Signaling Pathway

Xian-zong Ye,[*,†,1] Sen-lin Xu,[*,†,1] Yan-hong Xin,[*,†,1] Shi-cang Yu,[*,†] Yi-fang Ping,[*,†] Lu Chen,[*,†] Hua-liang Xiao,[*,†] Bin Wang,[*,†] Liang Yi,[‡] Qing-liang Wang,[*,†] Xue-feng Jiang,[*,†] Lang Yang,[*,†] Peng Zhang,[*,†] Cheng Qian,[*,†] You-hong Cui,[*,†] Xia Zhang,[*,†] and Xiu-wu Bian[*,†]

The invasion of malignant glioma cells into the surrounding normal brain tissues is crucial for causing the poor outcome of this tumor type. Recent studies suggest that glioma stem-like cells (GSLCs) mediate tumor invasion. However, it is not clear whether microenvironment factors, such as tumor-associated microglia/macrophages (TAM/Ms), also play important roles in promoting GSLC invasion. In this study, we found that in primary human gliomas and orthotopical transplanted syngeneic glioma, the number of TAM/Ms at the invasive front was correlated with the presence of CD133$^+$ GSLCs, and these TAM/Ms produced high levels of TGF-β1. CD133$^+$ GSLCs isolated from murine transplanted gliomas exhibited higher invasive potential after being cocultured with TAM/Ms, and the invasiveness was inhibited by neutralization of TGF-β1. We also found that human glioma-derived CD133$^+$ GSLCs became more invasive upon treatment with TGF-β1. In addition, compared with CD133$^-$ committed tumor cells, CD133$^+$ GSLCs expressed higher levels of type II TGF-β receptor (TGFBR2) mRNA and protein, and downregulation of TGFBR2 with short hairpin RNA inhibited the invasiveness of GSLCs. Mechanism studies revealed that TGF-β1 released by TAM/Ms promoted the expression of MMP-9 by GSLCs, and TGFBR2 knockdown reduced the invasiveness of these cells in vivo. These results demonstrate that TAM/Ms enhance the invasiveness of CD133$^+$ GSLCs via the release of TGF-β1, which increases the production of MMP-9 by GSLCs. Therefore, the TGF-β1 signaling pathway is a potential therapeutic target for limiting the invasiveness of GSLCs. ***The Journal of Immunology*****, 2012, 189: 444–453.**

Malignant gliomas are the most common primary brain tumors. Despite the improvement in therapy during the past 5 y, the median survival time for glioblastoma, the most aggressive glioma, is no more than 14 mo after diagnosis (1). The aggressive invasion by malignant glioma cells into surrounding normal brain tissues has increasingly been recognized as an important cause for frequent relapse that leads to high mortality (2). During the past decade, emerging evidence supports the notion that cancer stem cells (CSCs) or cancer-initiating cells are responsible for tumor development including invasion and angiogenesis, therapy resistance, and recurrence (3–6). Glioma stem-like cells (GSLCs) have been demonstrated to possess highly invasive activity (7, 8). Besides, the invasive glioma cells present stem cell characteristics with increasing neurosphere formation ability and tumorigenicity (4, 9). However, the effect of microenvironment or niche on GSLC invasion remains unclear.

The influence of tumor microenvironment on tumor progression has been emphasized for many years in almost all kinds of tumor, including glioma (10–12). Tumor-infiltrating leukocytes are mobilized and recruited by tumor-derived factors that contribute to the tumor microenvironment. Tumor-associated macrophages (TAMs), the distinct alternatively activated M2 polarized population, are the main components of tumor-infiltrating leukocytes (13–15), which are involved in tumor angiogenesis and invasion (14, 16). In addition to infiltrated leukocytes, resident cells including tissue macrophages such as microglia in the brain are also important contributors for tumor progression. Of note, one recent study suggests that TAMs, arising from peripheral monocytes rather than resident microglia, are the predominant inflammatory cells to infiltrate human gliomas (17). The biological significance and possible clinical implications of tumor-associated microglia/macrophages (TAM/Ms) in the marginal area of gliomas are not yet fully understood. Furthermore, the high activity of the TGF-β signaling pathway in human glioma tissues has been associated with a poor prognosis (18). Infiltrating leukocytes are responsible for the accumulation of TGF-β1 at the invasive front area of tumor, whereas glioma cells are reported to produce TGF-β2 (18–21). Once activated, TGF-β binds the type II TGF-β receptor (TGFBR2). The ligand-bound TGFBR2 is then able efficiently to *trans*-activate the type I TGF-β receptor (TGFBR1), which transduces intracellular signals through canonical Smad-dependent and/or Smad-independent pathways, such as ERK, p38, Rac, and PI3K–Akt pathways (19, 20, 22). TGFBR2 knockdown was

*Key Laboratory of Tumor Immunopathology, Third Military Medical University, Ministry of Education of China, Chongqing 400038, China; †Institute of Pathology and Southwest Cancer Center, Southwest Hospital, Third Military Medical University, Chongqing 400038, China; and ‡Department of Neurosurgery, Daping Hospital, Third Military Medical University, Chongqing 400038, China

[1]X.-z.Y., S.-l.X., and Y.-h.X. contributed equally to this work.

Received for publication November 17, 2011. Accepted for publication May 3, 2012.

This work was supported by grants from the National Basic Research Program of China (973 Program, 2010CB529403) and the National Natural Science Foundation of China (30725035, 30930103, and 30872297).

Address correspondence and reprint requests to Prof. Xiu-wu Bian and Prof. Xia Zhang, Institute of Pathology and Southwest Cancer Center, Southwest Hospital, Third Military Medical University, Gaotanyan 30, Shapingba District, Chongqing 400038, China. E-mail addresses: bianxiuwu@263.net (X.-w.B.) and zhangxia45@yahoo.com (X.Z.)

The online version of this article contains supplemental material.

Abbreviations used in this article: CSC, cancer stem cell; GSLC, glioma stem-like cell; IHC, immunohistochemistry; shRNA, short hairpin RNA; TAM, tumor-associated macrophage; TAM/M, tumor-associated microglia/macrophage; TGFBR1, type I TGF-β receptor; TGFBR2, type II TGF-β receptor; TGFBR3, type III TGF-β receptor.

Copyright © 2012 by The American Association of Immunologists, Inc. 0022-1767/12/$16.00

www.jimmunol.org/cgi/doi/10.4049/jimmunol.1103248

Downloaded from http://www.jimmunol.org/ by guest on August 4, 2022

shown to inhibit the invasion of glioma cells (23). The contributions of TGF-β to cancer development processes, such as cell invasion, immune suppression, and microenvironment modification, have been well recognized (1, 19, 20). Moreover, recent studies showed that TGF-β can increase self-renewal capability of GSLCs (21, 24). Whether and how the TGF-β signaling pathway contributes to other biological properties of GSLCs, such as invasion, remain to be explored.

In the current study, we aimed to understand the role of TAM/Ms during GSLC invasion with focus on the TGF-β1 signaling pathway. We found that in both human glioma samples and animal models, the distribution of TAM/Ms in the marginal area correlated with the location of CD133$^+$ glioma cells. GSLCs exhibited high invasive potential, especially in the presence of TAM/Ms without direct cell–cell contact. TGFBR2 coexpressed with CD133 in GSLCs was found to be responsible for TAM/Ms-mediated invasion of GSLCs. Furthermore, downregulation of TGFBR2 decreased the invasion of GSLCs both in vitro and in vivo. Our results indicate that TAM/Ms significantly enhance the invasive capability of GSLCs through paracrine production of TGF-β1 and the TGF-β1–TGFBR2 signaling pathway.

Materials and Methods

Patient glioma samples

Surgical glioma specimens were obtained from patients in the Department of Neurosurgery, Southwest Hospital and Daping Hospital, Third Military Medical University (Chongqing, China). Written informed consent to perform biological studies was obtained from all of the participants, and the study was approved by the Ethics Committee of the Southwest Hospital and Daping Hospital at Third Military Medical University. The tumors were classified by at least two pathologists according to the 2007 World Health Organization classification of CNS tumors (25).

Preparation of CD133$^+$ and CD133$^-$ cells

Murine glioma cell line GL261 was obtained from the German Cancer Research Center and as a gift from Prof. Zi-ling Wang (Beijing Institute of Transfusion Medicine, Beijing, China). GL261 and five cases of human primary glioma specimens were cultured in DMEM (Life Technologies) containing 10% FBS (Life Technologies). CD133$^+$ or CD133$^-$ populations were isolated by sorting from GL261 cell line and/or primary specimens using PE anti-mouse CD133 Ab (eBioscience) and PE anti-human CD133 Ab (Miltenyi Biotec, Bergisch-Gladbach, Germany), respectively. Before separation, the percentages of CD133$^+$ cells in the samples were assayed using the Abs described above and isotype controls. For sorting of CD133$^+$ and CD133$^-$ tumor cells from GL261-derived tumors, single-cell suspensions were prepared from GL261-derived tumors as described previously (26). Cells were then incubated for 10 min at 4°C with rat anti-mouse CD16/CD32 Ab (BD Pharmingen). Subsequently, cells were incubated for 30 min at 4°C with PE anti-mouse CD133 Ab (eBioscience). 7-Aminoactinomycin D (BD Pharmingen) was added (1:10) to discriminate between viable and dead cells. The purity of the cells after sorting was detected using flow cytometry. Data acquisition and analysis were performed on a BD FACSAria II using CellQuestPro software (BD Biosciences). Sorted CD133$^+$ tumor cells were maintained in stem cell medium, whereas CD133$^-$ tumor cells were cultured in DMEM supplemented with 10% FBS as previously described (27).

Tumor implantation

Three animal models were used in this study. All the animals were purchased from the Laboratory Animal Center, Third Military Medical University (Chongqing, China). In the first model, 1×10^6 GL261 cells or 1×10^6 CD133$^+$ cells were implanted s.c. into syngeneic C57BL/6 mice. Tumor-bearing mice were sacrificed 19 d after transplantation. TAMs and CD133$^+$ or CD133$^-$ tumor cells were analyzed or sorted as described earlier. In the second model, CD133$^+$ or CD133$^-$ cells sorted from GL261-derived tumors were injected orthotopically with cell numbers of either 1×10^3 or 1×10^4 per mouse into the brains of 6-wk-old female C57BL/6 mice, respectively (n = 5). CD133$^+$ tumor cells (2×10^4) infected with lentiviral stocks were transplanted orthotopically into the brains of 6-wk-old female C57BL/6 mice (n = 7). Mice were maintained up to 4 wk. In the third model, 1×10^3 CD133$^+$ or 5×10^5 CD133$^-$ tumor cells sorted from primary glioma specimens were injected orthotopically into the brains of 6-wk-old female NOD-SCID mice, respectively (n = 5). At 12–16 wk postinjection, these NOD-SCID mice were euthanized for analysis. The brains of C57BL/6 mice and NOD-SCID mice were collected for further analysis. The animal experiments were approved by the Institutional Animal Care and Use Committee of the Third Military Medical University.

Immunohistochemistry and immunofluorescence staining

Immunohistochemistry (IHC) was performed on paraffin sections of primary glioma specimens to investigate the distribution of stem cell marker-expressing glioma cells and TAM/Ms in the marginal area. Immunofluorescence staining was performed on the frozen sections of orthotopic GL261-derived tumors. Mouse anti-nestin (1:200; Chemicon), rabbit anti-Sox2 (1:200; Abcam, Cambridge, U.K.), and rabbit anti-CD133 (1:200; Abcam) were used as GSLCs markers. Rabbit anti-GFAP (1:100; Boster Biotech, Wuhan, China), rabbit anti-MBP (1:200; Millipore), and mouse anti–β-tubulin III (1:100; Chemicon) were used to identify astrocytic, oligodendrocytic, and neuronal phenotypes, respectively. Mouse anti-human CD68 (1:200; Abcam), rabbit anti-human CD163 (1:100; Abnova, Taipei, Taiwan), and rat anti-mouse CD11b (1:200; eBioscience) as well as rat anti-mouse F4/80 (1:100; eBioscience) were used as TAM/Ms markers for human and mice, respectively. Rabbit anti-TGFBR2 (1:200; Santa Cruz Biotechnology), goat anti-TGFBR2 (1:200; Santa Cruz Biotechnology), and mouse anti–TGF-β1 (1:200; Abcam) were also used. IHC and immunofluorescence staining was performed as previously described (28, 29).

Preparing TAM/Ms and CD11b$^+$F4/80$^+$ macrophages

The procedures for sorting CD11b$^+$F4/80$^+$ TAM/Ms from GL261-derived tumors were performed as described earlier. For sorting of macrophages from the spleens of tumor-free mice, C57BL/6 mouse spleens were sheared through a 200-mesh stainless steel sieve, and RBCs were lysed by red cell lysis buffer (Tiangen Biotech, Beijing, China) for 10 min at room temperature. Rat anti-mouse CD16/CD32 Ab (BD Pharmingen), FITC anti-mouse CD11b, PE anti-mouse F4/80 Abs (eBioscience), and 7-aminoactinomycin D (BD Pharmingen) were used in these experiments. The assay for purity and data acquisition and analysis were described earlier. Isolated splenic macrophages and TAM/Ms were cultured in RPMI 1640 (Life Technologies) supplemented with 5% FBS (PAA, Pasching, Australia) for 18 h as controls. Alternatively, 20 ng/ml IL-4 as well as 100 ng/ml LPS plus 20 ng/ml IFN-γ were used to stimulate these two types of macrophages, respectively, for 18 h as previously described (30). The supernatants were collected and stored at –80°C for ELISA. The cells were washed twice and prepared for extraction of total RNA.

Colony formation assay

Plate colony formation assay was used to evaluate the self-renewal ability of CD133$^+$ tumor cells. Freshly sorted CD133$^+$ tumor cells and their CD133$^-$ counterparts were seeded into 24-well plates at 300 cells per well, respectively. All samples were plated in triplicate. During colony growth, the culture medium was replaced every 4 d. After 2 wk, the plates were stained with crystal violet (0.2% in 2% ethanol) for 20 min, and the colonies containing more than 50 cells were counted.

Coculture of TAM/Ms with either CD133$^+$ or CD133$^-$ tumor cells

Sorted TAM/Ms (2×10^5 cells per insert) were seeded into upper inserts of Transwell cell culture chambers (6 wells, 0.4-μm pore size; Falcon, Oxnard, CA) and cocultured with the same number of CD133$^+$ or CD133$^-$ tumor cells (2×10^5 cells per well) in the lower chambers without direct contact. To verify the effect of TGF-β1 in the process of TAM/M-mediated GSLC invasion, the Ab blocking assay was performed. Briefly, TGF-β1 neutralizing Ab (1 μg/ml, mouse monoclonal anti−TGF-β1; Abcam) was incubated during CD133$^+$ and CD133$^-$ tumor cells coculture with TAM/Ms. CD133$^+$ or CD133$^-$ tumor cells alone were cultured in a 6-well plate as controls. Twenty-four hours from initiation of culture, upper inserts containing TAM/Ms were discarded. CD133$^+$ or CD133$^-$ tumor cells cocultured with or without TAM/Ms were washed and then used for subsequent experiments.

To enunciate the signaling pathway responsible for the biological activity of CD133$^+$ tumor cells after coculture with TAMs, several inhibitors were incubated with CD133$^+$ tumor cells before coculture with TAMs. The inhibitors were used at concentrations as follows: 10 μM SIS3, a specific inhibitor of Smad3; 10 μM LY294002, a specific inhibitor of PI3K; 10 μM PD98059, a specific inhibitor of MEK; and 50 μM NSC23766, a specific inhibitor of Rac. These inhibitors were purchased from Calbiochem (San Diego, CA). SB203580 (Sigma-Aldrich Chemical), a specific inhibitor of

Downloaded from http://www.jimmunol.org/ by guest on August 4, 2022

p38, was used at a concentration of 1 μM. All the inhibitors except PD98059 were preincubated with CD133$^+$ tumor cells for 1 h, and PD98059 was preincubated with CD133$^+$ tumor cells for 2 h.

Pretreatment of CD133$^+$ or CD133$^-$ tumor cells with TGF-β1

To define further the invasion-promoting effects of TGF-β1, CD133$^+$ or CD133$^-$ tumor cells (2×10^5 cells per well) sorted from primary glioma specimens were seeded into a 6-well plate with or without pretreatment with TGF-β1 (5 ng/ml; PeproTech, Rocky Hill, NJ). Twenty-four hours from initiation of culture, CD133$^+$ or CD133$^-$ tumor cells with or without pretreatment with TGF-β1 were washed and then used for subsequent experiments.

Invasion assay

The invasion assay was performed using Transwell cell culture chambers (24 wells, 8-μm pore size; Corning). Briefly, upper inserts were coated with 30 μl Matrigel (1:1 dilution; BD Biosciences), and then allowed to set for 30 min at 37°C. CD133$^+$ or CD133$^-$ tumor cells were harvested after 24 h of coculture with TAM/Ms or 24 h of pretreatment with TGF-β1. Then, 2×10^5 CD133$^+$ tumor cells or CD133$^-$ tumor cells were resuspended in 200 μl of serum-free DMEM and added to the corresponding upper inserts, respectively. DMEM (600 μl) with 10% FBS was added to the lower chamber. After 24 h, invaded cells were fixed and stained with crystal violet (0.2% in 2% ethanol) for 20 min. Cells on the upper side of the insert membrane were removed with cotton rods. The invaded cells were counted at a magnification of ×100 under a light microscope in nine different fields for each insert. The experiments were repeated at least three times.

TGFBR2 targeting short hairpin RNA

The short hairpin RNA (shRNA) sequences targeting murine TGFBR2 were designed using Invitrogen online BLOCK-iT RNAi Designer (http://www.invitrogen.com/rnai). A previously described nonsilencing sequence (5′-TTCTCCGAACGTGTCACGT-3′) was used as a control (31). The targeting sequences of shRNAs on TGFBR2 used in the experiments were 5′-CCAACAACATCAACCACAA-3′ (shRNA1), 5′-GGAGAAGATTCCAGAAGAT-3′ (shRNA2), 5′-CCTCACTGCTCACTCCTAA-3′ (shRNA3), and 5′-GCTTCGAACACCATGGAAA-3′ (shRNA4). The TGFBR2-targeting shRNA sequences or mock sequences were inserted into the pMagic4.1 expressing vector that expresses eGFP (SunBio, Shanghai, China). Lentiviral stocks were generated by transfecting the pMagic4.1 constructs expressing shRNA targeting TGFBR2 into 293T cells, followed by harvesting after 48 h. Efficiency of lentiviral-mediated shRNA knockdown of TGFBR2 in cells was determined by Western blot analysis and real-time PCR. The lentiviral stocks were used to infect CD133$^+$ and CD133$^-$ cells at a multiplicity of infection of 100. Cells stably expressing TGFBR2-targeting shRNA were sorted by FACS before they were cocultured with TAM/Ms.

Real-time PCR

Total RNA was extracted with RNAiso reagent (Takara, Dalian, China). Five hundred nanograms of RNA from each group was used for RT-PCR with a two-step RT-PCR kit (Takara). Real-time PCR was performed with Maxima SYBR Green/Rox qPCR Master Mix (Fermentas) to analyze the differential expressions of TGFBR1, TGFBR2, type III TGF-β receptor (TGFBR3), MMP-2, and MMP-9 in tumor cells and the cytokines levels in macrophages. The expression of GAPDH mRNA was determined for normalization. The cycling conditions were 5 min at 95°C, 40 cycles of 10 s at 95°C, 15 s at 60°C, 20 s at 72°C, and 5 s at 84°C. The sequences of the primer pairs will be disclosed upon request. Real-time PCR was performed in triplicate including non-template controls.

ELISA

The supernatants of macrophage culture were centrifuged before ELISA. IL-10, IL-12p40 (R&D Systems), and TGF-β1 (eBioscience) were measured using commercial ELISA kits according to the manufacturer's instructions. Assay sensitivities were 4 pg/ml for IL-10, 1.8 pg/ml for IL-12p40, and 9 pg/ml for TGF-β1.

Western blot analysis

Western blot was performed as described previously (32). Briefly, the proteins of CD133$^+$ and CD133$^-$ tumor cells were extracted by RIPA Lysis Buffer (Beyotime Biotech, Nantong, China) with protease inhibitor PMSF (Beyotime Biotech). Proteins were subjected to 10% SDS-PAGE and transferred onto polyvinylidene fluoride membranes (Millipore). The membranes were blocked with 5% milk and then incubated with rabbit anti-TGFBR2 (1:1000; Santa Cruz Biotechnology), rabbit anti-GAPDH (1:1500; Cell Signaling Technology), rabbit anti–MMP-9 (1:500; Cell Signaling Technology), and rabbit anti–β-actin (1:500; Cell Signaling Technology) Abs overnight at 4°C. Membranes were sufficiently washed and then incubated with appropriate HRP-conjugated secondary Abs for 2 h at room temperature. Proteins were detected by ECL detection reagent. Expressions of TGFBR2 or MMP-9 were normalized against GAPDH or β-actin.

Statistical analysis

All experiments were conducted at least three times. The statistical significance between testing and control groups was analyzed with SPSS 10.0 statistical software. When two groups were compared, the unpaired Student *t* test was used. For in vivo study, Kaplan–Meier curves and log-rank analysis were performed. A p value <0.05 was considered statistically significant.

Results

Presence of CD11b$^+$ microglia/macrophages in the marginal area of glioma correlates with the location of CD133$^+$ glioma cells

Either infiltrated leukocytes and/or their counterparts in residence, particularly macrophages, are implicated in the progression of solid tumors (13). Whether or not these tumor-associated cells have effects on the cancer stem-like cells remains elusive. We performed immunofluorescence staining on the frozen sections of orthotopic murine GL261-derived tumors to investigate the distribution of stem cell marker-expressing glioma cells and TAM/Ms. As shown in Fig. 1A, a relatively high number of CD11b$^+$ cells was found in the invasive front area of glioma, which was coincident with a corresponding increment of CD133$^+$ glioma cells; that is, GSLCs (Fig. 1A). Likewise, the relatively lower density of GSLCs was consistent with that of CD11b$^+$ cells in the marginal area (Fig. 1B). As shown in the representative images of Fig. 1A and 1B, when the presence of CD133$^+$ cells and CD11b$^+$ cells within a distance of 100 μm from the invasive edge of glioma were taken into account, 20 fields were used to determine the relationship between local distributions of CD11b$^+$ cells and GSLCs. Regression analysis revealed a positive linear correlation between these two cell types in the marginal area of glioma (Fig. 1C). Of note, most of these CD11b$^+$ cells were also F4/80$^+$ as examined by immunofluorescence staining (Fig. 1D–G). Flow cytometry analysis of CD11b$^+$ myeloid cells isolated from ectopic murine GL261-derived tumors also confirmed that they were both CD45$^+$ (Fig. 1H) and F4/80$^+$ (Fig. 1I). Taken together, our data indicate that these glioma-associated myeloid cells are macrophages; that is, TAMs and the existence of CD133$^+$ GSLCs is strongly correlated with the distribution of TAMs in the marginal area.

GSLC-associated macrophages produce significant amounts of TGF-β1

It has been widely reported that TAMs are functionally polarized to alternatively activated M2 macrophage in the tumor microenvironment (14). M2 macrophages are characterized by their high production of TGF-β1 and IL-10, two most important cytokines that often perform immunomodulatory functions (19, 20, 33). Indeed, as shown in Fig. 2A, a high level of TGF-β1 was detected in the microenvironment surrounding CD11b$^+$ GSLC-associated macrophages in the tumor where CD133$^+$ glioma cells were found. We then purified CD11b$^+$F4/80$^+$ macrophages by flow cytometry sorting from GL261-derived tumors to a purity of 94.6% (Supplemental Fig. 1A). These purified sorted GSLC-associated macrophages or TAMs could adhere to the bottom of plastic culture wells and presented a typical round or oval shape of macrophages (Supplemental Fig. 1B). Moreover, CD11b was also

Downloaded from http://www.jimmunol.org/ by guest on August 4, 2022

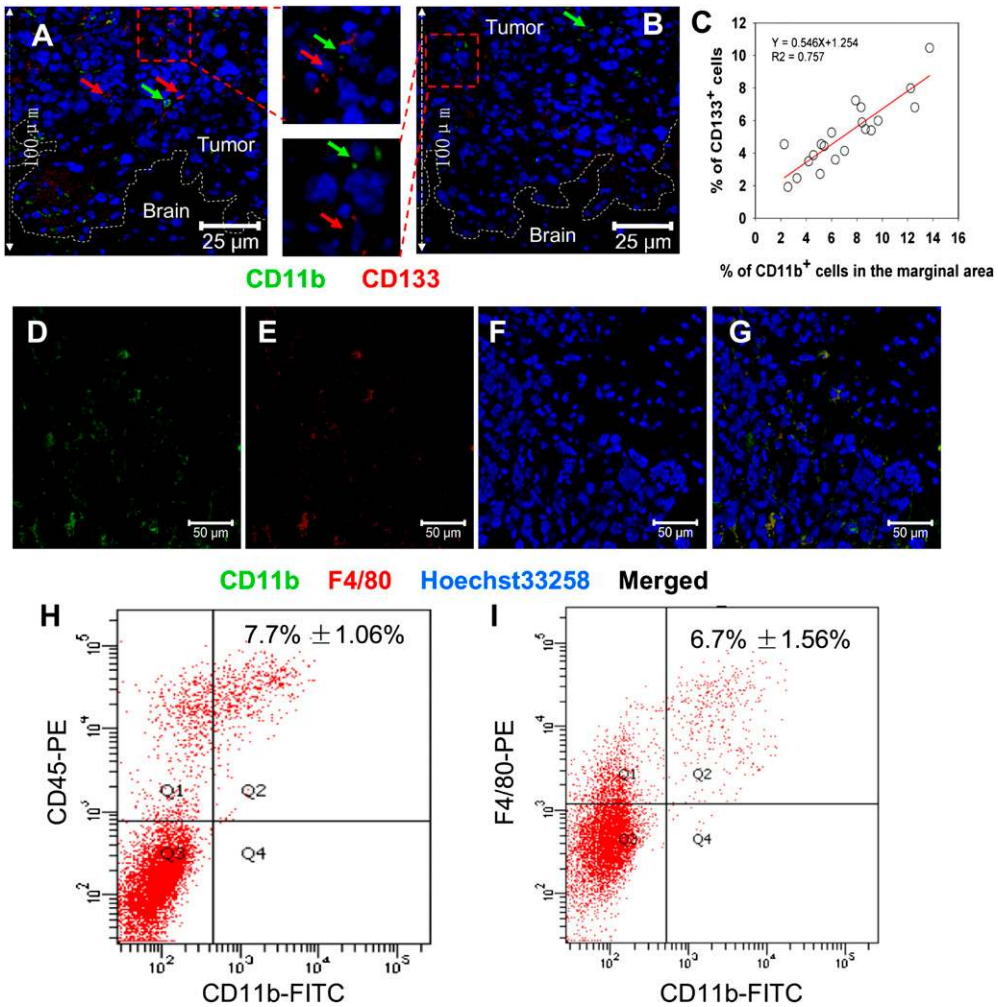

FIGURE 1. Presence of TAM/Ms in the marginal area of glioma correlates with CD133$^+$ glioma cells in murine orthotopically transplanted glioma. (**A** and **B**) The distribution of CD11b$^+$ macrophages (green) and CD133$^+$ glioma cells (red) in the invasive front area of orthotopic GL261 transplanted tumor. Nuclei were counterstained with Hoechst 33258 (blue). Immunofluorescence staining. (A) Relatively high numbers of both cell types. (B) Relatively low numbers of the both cell types. (**C**) Linear regression revealed a positive correlation between the distributions of CD11b$^+$ macrophages and CD133$^+$ glioma cells in murine glioma model. The relationship between local distributions of CD11b$^+$ cells and GSLCs was determined under 20 fields of confocal microscopy where CD133$^+$ cells and CD11b$^+$ cells were found within a distance of 100 μm from the invasive edge of glioma. (**D**–**G**) Distribution of CD11b$^+$/F4/80$^+$ macrophages in the murine orthotopic glioma. Representative immunofluorescence images of CD11b$^+$/F4/80$^+$ macrophages are presented. (D) CD11b (green). (E) F4/80 (red). (F) Nuclei were counterstained with Hoechst 33258 (blue). (G) Double positive for CD11b and F4/80 with Hoechst 33258-stained nuclei is shown in merge. (**H**) Flow cytometry showed the majority of CD11b$^+$ macrophages coexpressed CD45 (*upper right*). (**I**) Percentage of CD11b$^+$F4/80$^+$ TAMs in GL261-derived tumors. Values represent the mean ± SD of triplicate determinations, and the data represent one of three independent experiments.

observed on the surface of these TAMs under immunofluorescence microscopy (Supplemental Fig. 1C). In comparison with classically activated M1 macrophages, cytokine profiles of purified TAMs were examined. To generate classically activated M1 macrophages, regular macrophages were isolated from the spleens of tumor-free mice and then stimulated with 100 ng/ml LPS and 20 ng/ml IFN-γ for 18 h. It was reported that IL-4 played an important role in generating alternatively activated M2 macrophages (26). We therefore treated TAMs with or without 20 ng/ml IL-4 or 100 ng/ml LPS plus 20 ng/ml IFN-γ for 18 h, and the released cytokines and their mRNA levels were measured. TAMs treated with IL-4 were high in TGF-β1 compared with TAMs treated with LPS plus IFN-γ (Fig. 2B, 2C). Although IL-10 production from TAMs treated with IL-4 was similar to that from TAMs treated with LPS plus IFN-γ, IL-12p40 production was much higher in TAMs treated with LPS plus IFN-γ (Fig. 2D). Other cytokines such as IL-1β, IL-6, and TNF-α, were lower in TAMs treated with IL-4 than in TAMs treated with LPS plus IFN-γ (Supplemental Fig. 1D). These results indicate that TAMs in GL261-derived tumors are polarized to alternatively activated M2 macrophages by producing high amounts of TGF-β1, and TAMs are skewed to M1 phenotype in the presence of LPS plus IFN-γ by producing huge amounts of IL-12p40.

Culture and characterization of GSLCs

The CD133$^+$ GSLCs from primary malignant glioma specimens, glioma cell line GL261, and GL261-derived tumors were prepared by FACS sorting with the corresponding surface markers. The heterogeneous contents of CD133$^+$ cells, ranging from 0.1 to 14.6%, were exhibited in five cases of human primary glioma specimens (Supplemental Fig. 2A). Approximately 0.67% of CD133$^+$ cells were detected from the GL261 cell line (Supplemental Fig. 2B). Notably, CD133$^+$ cells significantly increased in GL261-derived tumors or GL261 CD133$^+$ cell-derived tumors, which were 1.84 or 2.05% of total cells, respectively (Supplemental Fig. 2B). Case 1 and case 2 of primary glioma specimens

Downloaded from http://www.jimmunol.org/ by guest on August 4, 2022

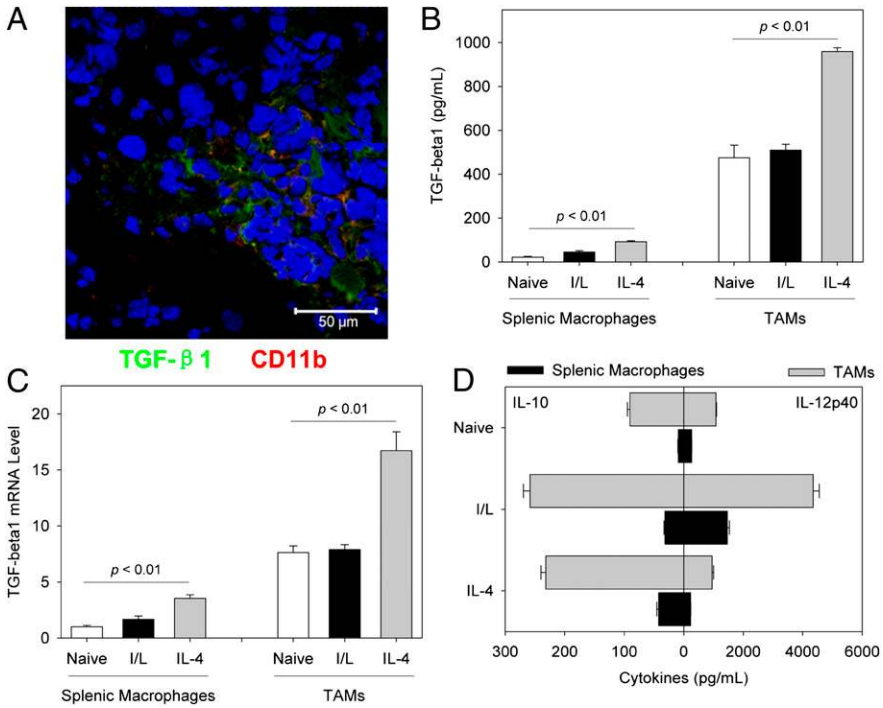

FIGURE 2. TGF-β1 expression in TAMs derived from murine transplanted glioma. (**A**) TGF-β1 cytokine (green) was detected in the extracellular matrix of CD11b$^+$ macrophages (red). Nuclei were counterstained with Hoechst 33258 (blue). Immunofluorescence staining. (**B**) TGF-β1 production from splenic macrophages and TAMs without stimulation (Naive) or stimulated with IFN-γ and LPS (I/L) or IL-4. (**C**) TGF-β1 mRNA level in the splenic macrophages and TAMs without stimulation (Naive) or stimulated with IFN-γ and LPS (I/L) or IL-4. (**D**) Production of IL-10 and IL-12p40 from splenic macrophages and TAMs without stimulation (Naive) or stimulated with IFN-γ and LPS (I/L) or IL-4. Data are the mean ± SD in triplicate, and one of three independent experiments is presented.

as well as GL261-derived tumors were chosen for sorting CD133$^+$ cells as they contained relatively higher numbers of CD133$^+$ cells. After sorting, the purified cells were evaluated by flow cytometry. The purities of CD133$^+$ cells in case 2 and GL261-derived tumors were more than 90% (Supplemental Fig. 2C). To establish colony formation capabilities of CD133$^+$ and CD133$^-$ cells, freshly sorted cells were seeded in 24-well plates at 300 cells per well. After 2-wk culture in DMEM supplemented with 10% FBS, CD133$^+$ cells displayed a higher capability for tumor colony formation than CD133$^-$ cells (Supplemental Fig. 2D). To examine tumor sphere-forming capabilities of CD133$^+$ and CD133$^-$ cells, freshly sorted cells from case 1, case 2, and GL261-derived tumors were seeded in serum-free neural stem cell medium. Neurospheres were formed by CD133$^+$ cells from all specimens at day 7 after initiation of culture (Supplemental Fig. 2E). The sorted CD133$^+$ cells expressed abundant nestin and Sox2 and lower level of GFAP. In contrast, CD133$^-$ cells contained very little nestin and Sox2 and high level of GFAP (Supplemental Fig. 3A). After culture in medium containing FBS 10% for 1 wk, CD133$^+$ cells exhibited multilineage differentiation potential, which was presented by high-level expressions of GFAP, MBP, and β-tubulin III (Supplemental Fig. 3B). To establish the tumorigenicity of CD133$^+$ cells, cells isolated from GL261-derived tumors were orthotopically implanted into C57BL/6, whereas cells isolated from primary glioma specimens were orthotopically implanted into NOD-SCID mice. Both showed high tumorigenicity. As few as 1×10^3 CD133$^+$ cells were able to initiate tumor formation. In contrast, 10-fold higher number of CD133$^-$ cells was needed to form tumor in C57BL/6 mice and 500-fold higher number of CD133$^-$ cells was required in NOD-SCID mice compared with that required for CD133$^+$ cells (Supplemental Table I). These results indicated that the CD133$^+$ cells from primary glioma specimens or GL261-derived tumors had higher tumorigenicity.

GSLC-associated macrophages enhance the invasive capability of GSLCs via TGF-β1

After obtaining GSLCs and macrophages from GL261-derived tumors by FACS sorting, we decided to compare the invasive ability of CD133$^+$ cells with that of CD133$^-$ cells as shown in Fig. 3. In monoculture conditions, CD133$^+$ cells displayed higher invasive ability than CD133$^-$ cells (Fig. 3A, d versus e, $p < 0.01$).

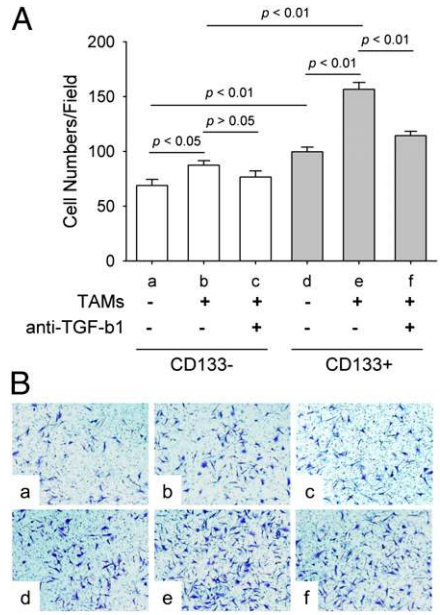

FIGURE 3. TAMs enhance invasiveness of glioma cells. (**A**) Comparing the invasive capabilities of CD133$^+$ and CD133$^-$ cells. The invasive capability of CD133$^+$ cells was higher than that of CD133$^-$ cells in monoculture conditions (**a** versus **d**, $p < 0.01$). The invasive capability of CD133$^+$ cells was increased notably after coculture with TAMs (d versus e, $p < 0.01$). The use of TGF-β1 neutralizing Ab in coculture system could significantly decrease the invasion of CD133$^+$ cells (**e** versus **f**, $p < 0.01$). In contrast, the invasive ability of CD133$^-$ cells only slightly decreased after the use of TGF-β1 neutralizing Ab (**b** versus **c**, $p > 0.05$). (**B**) Representative images for numbers of invasive cells in each group. Invaded cells were fixed and stained with crystal violet. Images were taken under light microscopy (original magnification ×10). Values represent the mean ± SD of triplicate determinations, and the data represent one of three independent experiments.

Downloaded from http://www.jimmunol.org/ by guest on August 4, 2022

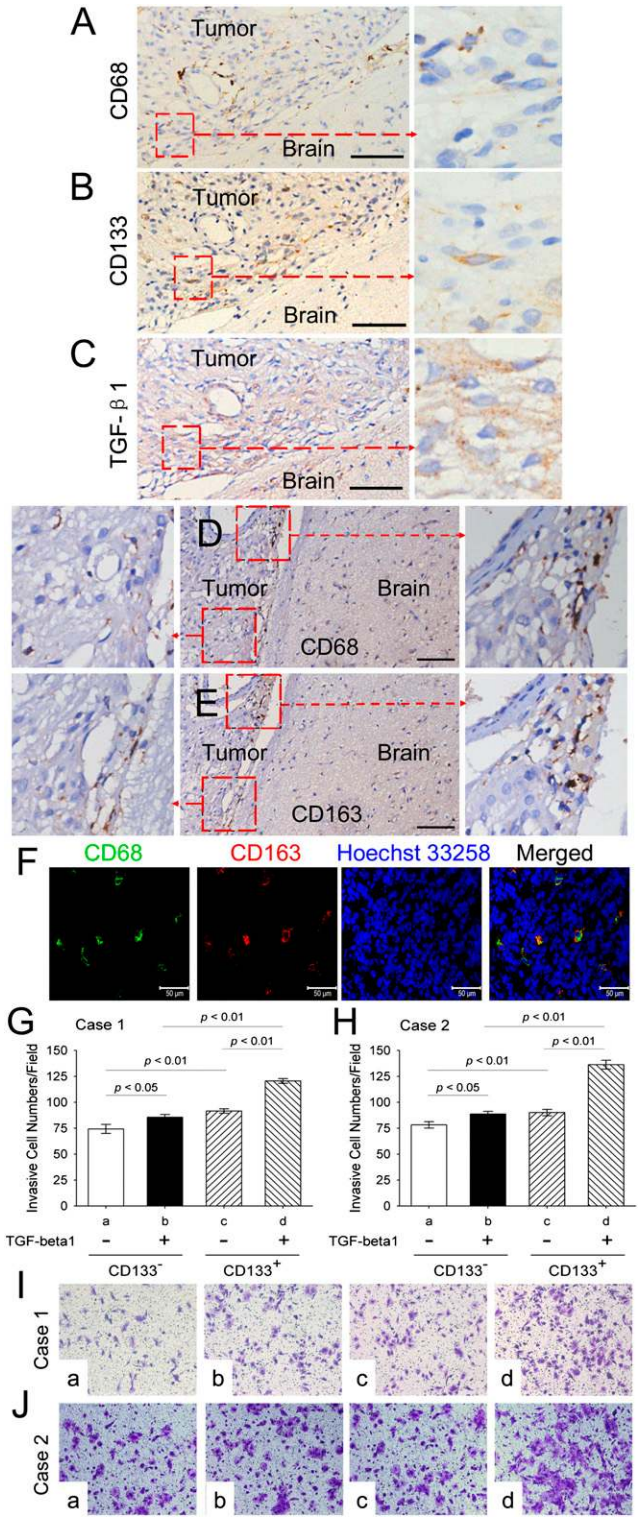

FIGURE 4. Association of CD68$^+$ macrophages with CD133$^+$ GSLCs in human glioblastoma. (**A**) A representative image of IHC staining showed the distribution of CD133$^+$ glioma cells (brown) in the marginal area of human glioblastoma. (**B**) A representative image of IHC staining showed a great number of CD68$^+$ macrophages (brown) located in the marginal area of human glioblastoma. (**C**) High level of TGF-β1 was detected in the microenvironment surrounding CD68$^+$ macrophages in human glioblastoma. (**D** and **E**) Representative IHC images of CD68$^+$ macrophages (D) that coexpress CD163 (E). The images were taken under light microscopy. Scale bar, 100 μm. (**F**) The coexpression of CD68 (green) and CD163 (red) Ags on the surface of infiltrating TAMs in human glioma specimens. Nuclei were counterstained with Hoechst 33258 (blue). Immunofluorescence staining. (**G** and **H**) Comparing the invasive capabilities of CD133$^+$ and CD133$^-$ cells. Comparing with CD133$^-$ cells, the invasion ability of CD133$^+$ cells from case 1 (G) and case 2 (H) was slightly increased without pretreatment with TGF-β1 (**a** versus **c** in case 1, $p < 0.01$; a versus c in case 2, $p < 0.05$). The invasive capability of CD133$^+$ cells was remarkably increased after pretreatment with TGF-β1 (c versus **d**, $p < 0.01$). (**I**) Representative images for each group of case 1 are presented. (**J**) Representative images for each group of case 2 are presented. Invaded cells were fixed and stained with crystal violet. Images were taken under light microscopy (original magnification ×10). Values represent the mean ± SD in triplicate, and the data represent one of three independent experiments.

In coculture system, macrophages sorted from GL261-derived tumors were seeded into the upper inserts of a 6-well Transwell and cocultured with the same number of CD133$^+$ cells or CD133$^-$ cells for 24 h. After coculture, GSLC-associated macrophages (i.e., TAMs) in the upper inserts were discarded, and CD133$^+$ cells and CD133$^-$ cells were assayed for invasion (Fig. 3). Comparing with CD133$^-$ cells, CD133$^+$ cells displayed notably increased invasive ability after coculture with TAMs (Fig. 3A, d versus e, $p < 0.01$).

To determine the role of TGF-β1 in the invasive process, TGF-β1 neutralizing Ab was applied in the cocultures. After the use of TGF-β1 neutralizing Ab in cocultures, the invasiveness of CD133$^+$ cells was significantly reduced (Fig. 3A, e versus f, $p < 0.01$). In contrast, the invasive ability of CD133$^-$ cells only slightly decreased (Fig. 3A, b versus c, $p > 0.05$). These results suggested that TGF-β1 derived from GSLC-associated macrophages was critical in increasing the invasive potential of CD133$^+$ glioma cells.

Presence of human CD68$^+$ macrophages in the invasive front area of human glioma correlates with the location of CD133$^+$ glioma cells

We next addressed whether there was association of microglia or macrophages with glioma in the primary glioma surgically removed from patients. Serial paraffin sections of primary human glioma specimens were analyzed to study the correlation of CD68$^+$ macrophages and CD133$^+$ glioma cells as shown in Fig. 4. IHC staining of these sections showed CD133$^+$ glioma cells located at the invasive front area of glioma (Fig. 4A). CD68$^+$ macrophages in the marginal area of glioma were accompanied by increasing numbers of CD133$^+$ glioma cells (Fig. 4B). Furthermore, TGF-β1 was detected in the microenvironment containing CD68$^+$ macrophages (Fig. 4C). We also observed that most CD68$^+$ macrophages coexpressed CD163, a marker for M2 phenotype (Fig. 4D–F). These results suggest that TGF-β1–expressing TAM/Ms may be associated with GSLC invasion.

To address further whether TGF-β1 could contribute to the invasive capability of CD133$^+$ glioma cells, we added TGF-β1 to the CD133$^+$ cells or CD133$^-$ cells that were isolated from primary glioma specimens from two patients (Supplemental Fig. 2) and then examined their invasive capabilities. Not surprisingly, we found that CD133$^+$ cells displayed higher invasive ability than CD133$^-$ cells without pretreatment with TGF-β1 (Fig. 4G, 4I: case 1: a versus c, $p < 0.01$; Fig. 4H, 4J: case 2: a versus c, $p < 0.01$). Invasive capabilities of CD133$^+$ cells of primary gliomas from two different patients were found remarkably increased after preincubation with TGF-β1 for 24 h (Fig. 4G, 4H: c versus d, $p < 0.01$). These results indicate that TGF-β1 can promote GSLC invasiveness in vitro.

MMP-9 but not MMP-2 is the major contributor for GSLC invasiveness

MMPs such as MMP-2 and MMP-9 are known to be associated with glioma invasion, and these enzymes are reportedly induced by

Downloaded from http://www.jimmunol.org/ by guest on August 4, 2022

TGF-β1 (34, 35). To delineate further the invasion promotion effect of TAM-derived TGF-β1, the expression levels of MMP-2 and MMP-9 were determined by real-time PCR. As shown in Fig. 5A, the changes of MMP-2 mRNA expression were not significant in CD133$^+$ and CD133$^-$ cells, whereas MMP-9 expression was found ~7-fold higher in CD133$^+$ cells than in CD133$^-$ cells. Furthermore, in the presence of TAMs, additional increase of MMP-9 mRNA was detected in the CD133$^+$ GSLCs derived from orthotopic gliomas. TAMs had no effect on the expression of MMP-2 mRNA in both CD133$^+$ and CD133$^-$ tumor cells. Neutralization of TGF-β1 by TGF-β1 neutralizing Ab resulted in a reduction of MMP-9 mRNA in CD133$^+$ tumor cells (Fig. 5A).

The expressions of MMP-2 and MMP-9 mRNAs were also examined in the glioma specimens from two patients. As shown in Fig. 5B, in agreement with the findings from the above-mentioned study of murine GL261-derived tumors, MMP-2 expression was very low in both CD133$^+$ and CD133$^-$ cells, whereas MMP-9 expression was much higher in CD133$^+$ but low in CD133$^-$ glioma cells. Furthermore, the exogenous TGF-β1 significantly promoted MMP-9 expression in CD133$^+$ cells but had less effect on CD133$^-$ tumor cells (Fig. 5B). Notably, exogenous TGF-β1 had no significant effect on MMP-2 expressions in both CD133$^+$ and CD133$^-$ tumor cells (Fig. 5B). Previous studies suggest that Smad and MAPK–p38 pathways as well as others could be the integrated components in TGF-β1 signaling. Thus, TGF-β1–induced MMP-9 expression and invasiveness of CD133$^+$ tumor cells were examined in the presence of SIS3, an inhibitor for Smad3, and SB203580, a specific inhibitor of MAPK–p38 pathway. As shown in Fig. 5C and 5D, the inducible effects of TGF-β1 on MMP-9 expression and invasive capability of CD133$^+$ tumor cells were blocked by these two inhibitors, whereas inhibitors for other signaling pathways such as PD98059 (MEK1/2 inhibitor), LY294002 (PI3K inhibitor), and NSC23766 (Rac inhibitor) had very minor or no effect at all (data not shown). These results suggest that MMP-9 expression on CD133$^+$ cells mediated by TAM/M-derived TGF-β1 contributes to the high invasive capability of GSLCs, and inhibitors for Smad3 and MAPK–p38 pathways would be candidate drugs to treat glioma.

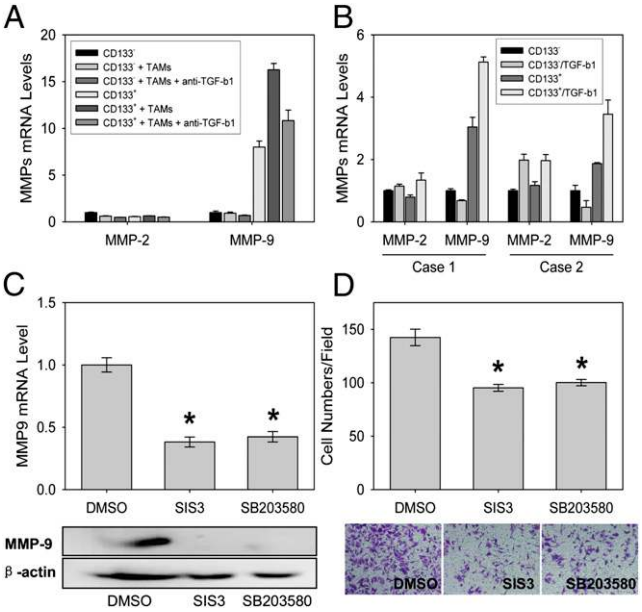

FIGURE 5. High expression of MMP-9 contributes to invasiveness of CD133$^+$ glioma cells. (**A**) The expression levels of MMP-2 and MMP-9 mRNA in CD133$^+$ cells and CD133$^-$ cells sorted from GL261-derived tumors after coculture with TAMs. (**B**) The expression levels of MMP-2 and MMP-9 mRNA in CD133$^+$ cells and CD133$^-$ cells sorted from primary glioma specimens after pretreatment with TGF-β1. (**C**) MMP-9 mRNA expression (*top*) and protein level (*bottom*) in the CD133$^+$ cells from GL261-derived tumors were reduced in the presence of SIS3 or SB203580. (**D**) Either SIS3 or SB203580 significantly reduced invasiveness of CD133$^+$ cells from GL261-derived tumors. Quantitative analysis (*top*); representative images (*bottom*). Invaded cells were fixed and stained with crystal violet; images were taken under light microscopy (original magnification ×10). Values represent the mean ± SD of triplicate determinations, and the data represent one of three independent experiments. *$p < 0.01$.

High level of TGFBR2 in CD133$^+$ GSLCs

To explore further the underlying mechanism by which TGF-β1 mediated GSLCs invasion, we examined the expression of three TGF-β1 receptors, TGFBR1, TGFBR2, and TGFBR3. The mRNA levels of these three receptors were measured by real-time PCR. As shown in Fig. 6A, TGFBR2 expression was found to be much higher in CD133$^+$ cells than that in CD133$^-$ cells from murine GL261-derived tumors. Next, we examined the expression of TGFBR2 in two human primary glioma samples. Similar to what

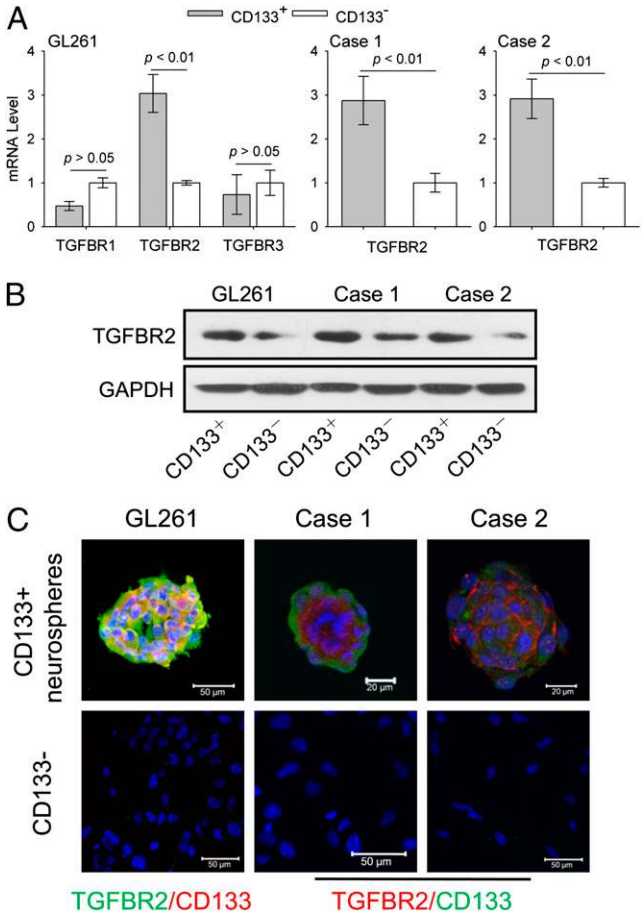

FIGURE 6. High level of TGFBR2 coexpressed with CD133 in GSLCs. (**A**) TGFBR1, TGFBR2, and TGBFR3 mRNA expression levels in CD133$^+$ and CD133$^-$ cells sorted from GL261-derived tumors (GL261); TGFBR2 mRNA expression levels in CD133$^+$ and CD133$^-$ cells sorted from human primary glioma specimens (Case 1 and Case 2). (**B**) TGFBR2 protein expression levels in CD133$^+$ cells and CD133$^-$ cells. (**C**) The coexpression of TGFBR2 and CD133 on neurospheres derived from CD133$^+$ cells (*top*) and on CD133$^-$ cells (*bottom*) were detected by immunofluorescence staining. Nuclei were counterstained with Hoechst 33258 (blue). Values represent the mean ± SD of triplicate determinations, and the data represent one of three independent experiments.

Downloaded from http://www.jimmunol.org/ by guest on August 4, 2022

we observed in murine GL261-derived tumors, TGFBR2 expression was higher in human CD133$^+$ cells but not CD133$^-$ cells (Fig. 6A). In parallel to their mRNA levels, higher protein level of TGFBR2 was detected in the CD133$^+$ cells derived from both human glioma samples and murine GL261-derived tumors than that in their CD133$^-$ counterparts (Fig. 6B). Furthermore, immunofluorescence double staining also confirmed the coexpression of TGFBR2 and CD133 in the neurospheres derived from CD133$^+$ cells that were isolated from GL261 and the samples from two patients, respectively, whereas the expressions of TGFBR2 and CD133 were significantly lower in CD133$^-$ tumor cells (Fig. 6C). Taken together, these data indicate that TGFBR2 is the key receptor for TGF-β1–mediated GSLC invasion.

Disruption of the TGF-β1 signaling pathway by knocking down TGFBR2 reduces the invasion capability of GSLCs

To determine whether the invasive process of GSLCs was contributed to by the TGFBR2 pathway, four pairs of murine-specific TGFBR2 shRNAs were individually transfected into CD133$^+$ or CD133$^-$ cells that were derived from GL261 tumors to knock down endogenous TGFBR2. TGFBR2 mRNA in CD133$^+$ tumor cells transfected with lentiviral stocks expressing shRNA1, shRNA2, shRNA3, or shRNA4 were reduced by 61.3, 70.2, 47.9, or 54.6%, respectively (Fig. 7A). Because TGFBR2 protein was remarkably decreased in the CD133$^+$ tumor cells that were transduced with shRNA2 (Fig. 7A, *inset*), we therefore chose shRNA2 for the next experiments. As shown in Fig. 7B, although TGFBR2 knockdown in CD133$^-$ cells had no effect on their invasion capability, CD133$^+$ tumor cells for which TGFBR2 was knocked down after transduction of shRNA2 significantly lost their invasive capability when they were cocultured with TAMs. Loss of invasiveness capability of the CD133$^+$ cells with TGFBR2 knockdown was correlated to the significant reduction of MMP-9 expression in these cells (Fig. 7C). These CD133$^+$ tumor cells with TGFBR2 knockdown were then injected orthotopically into the brains of C57BL/6 mice to examine their capability of growth in situ. Mice that were orthotopically implanted with CD133$^+$ tumor cells with TGFBR2 knockdown exhibited significantly prolong survival time by 5 to 7 d (Fig. 7D, $p < 0.05$). The invasion of glioma into surrounding normal brain tissue was examined at 3 wk after injection with immunofluorescence microscopy. As shown in Fig. 7E and 7F, the invasion of glioma derived from injection was significantly decreased. CD133$^+$ cells were remarkably reduced in the marginal area of transplanting tumors derived from TGFBR2 knockdown cells (Fig. 7G, mock versus shRNA2, $p < 0.01$). Thus, our data demonstrate that the reduction of TGFBR2 and disruption of TGF-β1 signaling pathway leads to the decreased invasive capability of CD133$^+$ tumor cells both in vitro and in vivo.

Discussion

In our previous work, we demonstrated a positive correlation between the participation of TAM/Ms and the density of GSLCs and confirmed that GSLCs played an important role in the recruitment of TAMs (29). In the current study, we examined whether TAM/Ms contributed to the invasion of GSLCs. By examining both human primary glioma samples and murine glioma xenograft, we observed that TAM/Ms were heavily distributed at the invasive front area of glioma, which was correlated with CD133$^+$ glioma cells (i.e., GSLCs). These TAM/Ms produced high amounts of TGF-β1. Moreover, we found that GSLCs had enhanced invasive ability after coculture with TAM/Ms or pretreatment with exogenous TGF-β1. Finally, we determined that

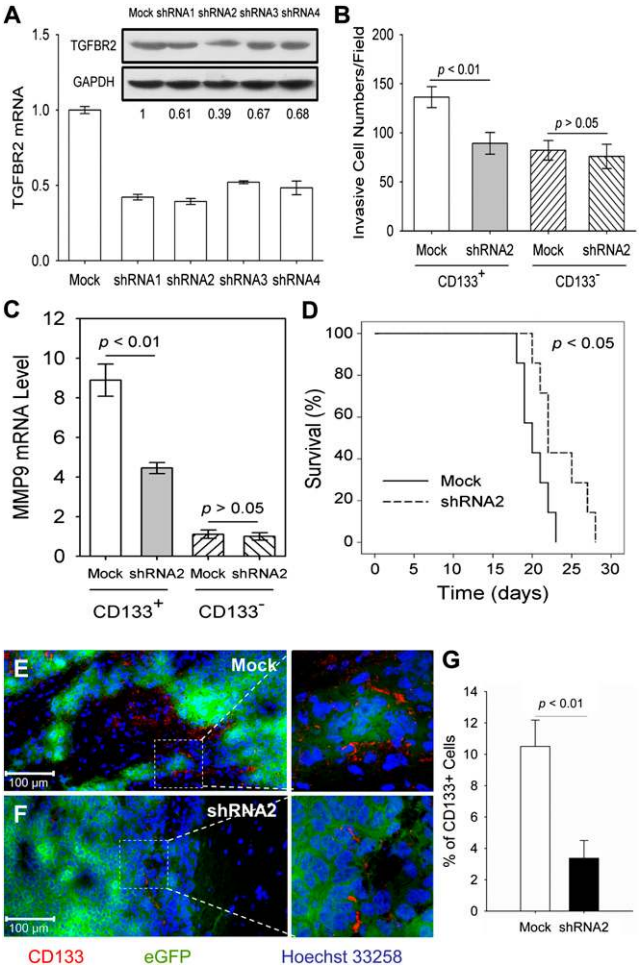

FIGURE 7. Knockdown of TGFBR2 by shRNA significantly reduces the expression of MMP-9 and inhibits the invasion capability of GSLCs. (**A**) TGFBR2 mRNA expression in the cells infected with mock, shRNA1, shRNA2, shRNA3, and shRNA4. All shRNAs remarkably downregulated TGFBR2 mRNA expressions and its protein level (*inset*). shRNA2 was the strongest one, and the other shRNAs had less effect. Values represent the mean ± SD of triplicate determinations, and the data represent one of three independent experiments. (**B**) shRNA2 significantly inhibited the invasive capability of CD133$^+$ cells but not CD133$^-$ cells. Mock of shRNA exhibited no effect on the invasive capabilities in both CD133$^+$ and CD133$^-$ cells. Values represent the mean ± SD of triplicate determinations, and the data represent one of three independent experiments. (**C**) The mRNA expressions of MMP-9 in CD133$^+$ cells and CD133$^-$ cells infected with mock or shRNA2 after coculture with TAMs. shRNA2 significantly inhibited MMP-9 mRNA expression of CD133$^+$ cells but had no effect on that of CD133$^-$ cells. Values represent the mean ± SD of triplicate determinations, and the data represent one of three independent experiments. (**D**) Knockdown of TGFBR2 decreased oncogenic potential of GSLCs and increased the survival of mice bearing intracranial GL261 tumors. Kaplan–Meier curves demonstrated increased survival time with TGFBR2 knockdown in C57BL/6 mice injected with 2×10^4 GSLC-infected lentiviral stocks. One representative from three independent experiments is shown (seven mice per group). (**E** and **F**) The invasion of CD133$^+$ cells (red) infected with mock and shRNA2 into surrounding normal brain tissues in vivo. Knockdown of TGFBR2 inhibited the invasion of glioma cells (eGFP, green), especially the CD133$^+$ glioma cells (green in plasma and red in cell membrane). Nuclei were counterstained with Hoechst 33258 (blue). Immunofluorescence staining. (**G**) The invasive ability of CD133$^+$ cells infected with shRNA2 was significantly decreased in vivo ($p < 0.01$). Quantitation of invading CD133$^+$ cells was determined under 5 fields of confocal microscopy where the CD133$^+$/eGFP$^+$ glioma cells were found within a distance of 100 μm from the invasive edge. Values represent the mean ± SD of triplicate determinations, and the data represent one of three independent experiments.

Downloaded from http://www.jimmunol.org/ by guest on August 4, 2022

the elevated production of MMP-9 from CD133$^+$ GSLCs by paracrine TGF-β1 from TAM/Ms via TGFBR2 pathway was the key contributor to the enhanced invasive potential of GSLCs.

The tumor microenvironment is indispensable for tumor initiation and progression (36). As the major contributing factor to the acquisition of core hallmark capabilities (e.g., angiogenesis, invasion, and metastasis) and the creation of a procancer microenvironment, inflammation is considered to be an enabling characteristic of cancer (12). Among tumor-infiltrating immune cells, TAMs are the major composition of the inflammation-related microenvironment in tumor (13, 14). Actually, TAMs infiltrate into the tumor lesion even in an early stage of tumorigenesis (37). The mechanisms responsible for the infiltration of TAMs into the tumor mass have been widely studied (16, 38). Regarding the malignant glioma, both the resident microglia and the macrophages derived from circulating monocytes constitute the glioma-infiltrating immune cells and are the major participants in glioma progression (39). Microglial cells play a dominant role in the early stage, whereas the macrophages derived from circulating monocytes are the major participant in the later stage to promote glioma growth (39). Thus, it would be possible to deter glioma from uncontrolled growth through intervening in the recruitment of circulating monocytes into the glioma mass. Moreover, the infiltrating TAM/Ms are considered to be immunosuppressive (M2) phenotype. GSLCs contribute greatly to the M2 polarization by a variety of secreted factors (40, 41).

According to Paget's "seed and soil" theory, the tumor microenvironment provides the appropriate "soil" or niche that is required for tumor cells, especially CSCs, to proliferate and disseminate (12, 42). Therefore, it is important to investigate the impact of the tumor microenvironment on CSCs (20, 43, 44). Tumor-infiltrating immune cells, such as Foxp3$^+$ regulatory T cells and TAMs, as well as the condition medium of macrophages, have been reported to drive the development and growth of CSCs (45–47). The dynamic cross talk between the tumor microenvironment and CSCs orchestrates tumor initiation and progression, and the aggressive invasion into surrounding normal brain tissues is a unique property of malignant glioma. The question raised here is whether TAM/Ms affect the invasion capability of GSLCs. Thus, we examined the distribution of GSLCs in both human primary glioma tissues and murine orthotopic GL261-derived tumors. Abundant GSLCs were found in the marginal area of glioma, and a large amount of TAM/Ms were clustered in the invasive front area of both primary glioma specimens and murine glioma model. TAM/Ms were associated with distribution of GSLCs at the invasive front area of glioma, accompanied by high production of TGF-β1. These results are in accord with previous reports that CSCs from many kinds of tumors exhibit high invasive ability and TAMs are recruited to the invasive site to enhance tumor invasion (7, 43, 48, 49). Thus, we hypothesize that TAM/Ms promote GSLC invasion through paracrine TGF-β1.

In accord with previous reports (13, 40), we found that glioma-infiltrating TAM/Ms are polarized to M2 phenotype by releasing high levels of immunosuppressive cytokines, such as IL-10 and TGF-β1. Glioma had been reported to secret IL-4, an important regulator of M2 polarization (26, 50), so we further detected the expression levels of immunosuppressive cytokines in TAMs and splenic macrophages in the presence of IL-4 or LPS plus IFN-γ. We found that TGF-β1 production from TAMs remained unchanged in the presence of LPS plus IFN-γ, whereas IL-10 production from TAMs treated with LPS plus IFN-γ was similar to that from TAMs treated with IL-4. However, TAMs treated with LPS plus IFN-γ produced huge amounts of IL-12p40 and expressed high levels of IL-1β, IL-6, and TNF-α, hallmarks of M1 polarization. Thus, TAMs are able to be skewed toward M1 phenotype in the presence of LPS plus IFN-γ.

Furthermore, we demonstrated that GSLCs possessed high invasive ability, especially after coculture with TAMs that were derived from transplanted tumors or pretreatment with exogenous TGF-β1. Previously, we and others found that GSLCs possessed high invasive ability (4, 51). The effect of TAMs to promote tumor invasion has been reported in the literature (12, 52). TAMs have been demonstrated to facilitate the tumor cell invasion by increasing a broad array of MMPs that can degrade proteins of the extracellular matrix (37, 53). Direct evidence has been presented that MMP-9 derived from bone marrow cells contributes to skin carcinogenesis (54). Additionally, TAMs also produce factors such as TGF-β1 and IL-10 that may enhance tumor immune suppression and facilitate tumor progression (40, 53). Several reports illustrate the role of TGF-β1 in maintaining the self-renewal property of GSLCs (21, 24). Tang and colleagues (55) reported that TGF-β1 could induce migration of mesenchymal stem cells. Recent study showed that treatment of TGF-β Ab reduced the invasion of glioma cells into surrounding normal brain in animal models (56). Our data showed that TGF-β1 from TAM/Ms promoted GSLC invasion. A decreased invasive ability was observed in CD133$^+$ tumor cells where TGF-β1 was neutralized. This provided a new insight into the role of TGF-β1 signaling in GSLC invasion.

TGFBR2 expression is higher in GSLCs compared with that in CD133$^-$ tumor cells. Knockdown of TGFBR2 expression in GSLCs significantly decreases the invasiveness of GSLCs even when they are cocultured with TAMs, indicating that TGFBR2 plays a critical role to mediate glioma invasion. MMP-2 and MMP-9 are known to be induced by the activation of TGF-β1 signaling (34, 35). We established that MMP-9 but not MMP-2 was the major effector responsible for GSLC invasion. Our results revealed that the MMP-9–dependent GSLC invasion was dependent on TAM/M-derived TGF-β1. Knockdown of TGFBR2 in CD133$^+$ tumor cells prolonged the survival time of animals transplanted with these cells. Transplant tumor derived from CD133$^+$ tumor cells with knockdown of TGFBR2 possesses remarkably decreased invasive ability, indicating the role of TGFBR2 in the TGF-β1–enhanced glioma invasion.

In summary, our study addresses the importance of the tumor microenvironment in glioma invasion. We demonstrate that TAMs infiltrating the marginal area of glioma and TGF-β1–TGFBR2 pathway are the key contributors for enhancing the invasion of GSLCs thereby promoting glioma progression. Development of therapeutic strategies against the TGF-β1–TGFBR2 signaling pathway and exploration of effective means for conversion of tumor-infiltrating macrophages into anti-tumor M1 phenotype may present new countermeasures to disrupt glioma invasion.

Acknowledgments

We thank Wei Sun and Li-ting Wang (Central Laboratory, Third Military Medical University, Chongqing, China) for technical assistance in laser confocal scanning microscopy.

Disclosures

The authors have no financial conflicts of interest.

References

1. Van Meir, E. G., C. G. Hadjipanayis, A. D. Norden, H. K. Shu, P. Y. Wen, and J. J. Olson. 2010. Exciting new advances in neuro-oncology: the avenue to a cure for malignant glioma. *CA Cancer J. Clin.* 60: 166–193.
2. Zagzag, D., K. Salnikow, L. Chiriboga, H. Yee, L. Lan, M. A. Ali, R. Garcia, S. Demaria, and E. W. Newcomb. 2005. Downregulation of major histocompatibility complex antigens in invading glioma cells: stealth invasion of the brain. *Lab. Invest.* 85: 328–341.

Downloaded from http://www.jimmunol.org/ by guest on August 4, 2022

3. Reya, T., S. J. Morrison, M. F. Clarke, and I. L. Weissman. 2001. Stem cells, cancer, and cancer stem cells. *Nature* 414: 105–111.
4. Molina, J. R., Y. Hayashi, C. Stephens, and M. M. Georgescu. 2010. Invasive glioblastoma cells acquire stemness and increased Akt activation. *Neoplasia* 12: 453–463.
5. Bao, S., Q. Wu, R. E. McLendon, Y. Hao, Q. Shi, A. B. Hjelmeland, M. W. Dewhirst, D. D. Bigner, and J. N. Rich. 2006. Glioma stem cells promote radioresistance by preferential activation of the DNA damage response. *Nature* 444: 756–760.
6. Yao, X. H., Y. F. Ping, J. H. Chen, C. P. Xu, D. L. Chen, R. Zhang, J. M. Wang, and X. W. Bian. 2008. Glioblastoma stem cells produce vascular endothelial growth factor by activation of a G-protein coupled formylpeptide receptor FPR. *J. Pathol.* 215: 369–376.
7. Inoue, A., H. Takahashi, H. Harada, S. Kohno, S. Ohue, K. Kobayashi, H. Yano, J. Tanaka, and T. Ohnishi. 2010. Cancer stem-like cells of glioblastoma characteristically express MMP-13 and display highly invasive activity. *Int. J. Oncol.* 37: 1121–1131.
8. Reddy, E. M., S. T. Chettiar, N. Kaur, R. Ganeshkumar, V. Shepal, N. C. Shanbhag, and A. Shiras. 2011. Dlxin-1, a member of MAGE family, inhibits cell proliferation, invasion and tumorigenicity of glioma stem cells. *Cancer Gene Ther.* 18: 206–218.
9. Yu, S. C., and X. W. Bian. 2009. Enrichment of cancer stem cells based on heterogeneity of invasiveness. *Stem Cell Rev.* 5: 66–71.
10. Hwang, R. F., T. Moore, T. Arumugam, V. Ramachandran, K. D. Amos, A. Rivera, B. Ji, D. B. Evans, and C. D. Logsdon. 2008. Cancer-associated stromal fibroblasts promote pancreatic tumor progression. *Cancer Res.* 68: 918–926.
11. Hoelzinger, D. B., T. Demuth, and M. E. Berens. 2007. Autocrine factors that sustain glioma invasion and paracrine biology in the brain microenvironment. *J. Natl. Cancer Inst.* 99: 1583–1593.
12. Hanahan, D., and R. A. Weinberg. 2011. Hallmarks of cancer: the next generation. *Cell* 144: 646–674.
13. Mantovani, A., and A. Sica. 2010. Macrophages, innate immunity and cancer: balance, tolerance, and diversity. *Curr. Opin. Immunol.* 22: 231–237.
14. Qian, B. Z., and J. W. Pollard. 2010. Macrophage diversity enhances tumor progression and metastasis. *Cell* 141: 39–51.
15. Solinas, G., S. Schiarea, M. Liguori, M. Fabbri, S. Pesce, L. Zammataro, F. Pasqualini, M. Nebuloni, C. Chiabrando, A. Mantovani, and P. Allavena. 2010. Tumor-conditioned macrophages secrete migration-stimulating factor: a new marker for M2-polarization, influencing tumor cell motility. *J. Immunol.* 185: 642–652.
16. Du, R., K. V. Lu, C. Petritsch, P. Liu, R. Ganss, E. Passegué, H. Song, S. Vandenberg, R. S. Johnson, Z. Werb, and G. Bergers. 2008. HIF1alpha induces the recruitment of bone marrow-derived vascular modulatory cells to regulate tumor angiogenesis and invasion. *Cancer Cell* 13: 206–220.
17. Parney, I. F., J. S. Waldron, and A. T. Parsa. 2009. Flow cytometry and in vitro analysis of human glioma-associated macrophages. Laboratory investigation. *J. Neurosurg.* 110: 572–582.
18. Bruna, A., R. S. Darken, F. Rojo, A. Ocaña, S. Peñuelas, A. Arias, R. Paris, A. Tortosa, J. Mora, J. Baselga, and J. Seoane. 2007. High TGFbeta-Smad activity confers poor prognosis in glioma patients and promotes cell proliferation depending on the methylation of the PDGF-B gene. *Cancer Cell* 11: 147–160.
19. Massagué, J. 2008. TGFbeta in Cancer. *Cell* 134: 215–230.
20. Bierie, B., and H. L. Moses. 2010. Transforming growth factor beta (TGF-beta) and inflammation in cancer. *Cytokine Growth Factor Rev.* 21: 49–59.
21. Peñuelas, S., J. Anido, R. M. Prieto-Sánchez, G. Folch, I. Barba, I. Cuartas, D. García-Dorado, M. A. Poca, J. Sahuquillo, J. Baselga, and J. Seoane. 2009. TGF-beta increases glioma-initiating cell self-renewal through the induction of LIF in human glioblastoma. *Cancer Cell* 15: 315–327.
22. Zhang, Y. E. 2009. Non-Smad pathways in TGF-beta signaling. *Cell Res.* 19: 128–139.
23. Wesolowska, A., A. Kwiatkowska, L. Slomnicki, M. Dembinski, A. Master, M. Sliwa, K. Franciszkiewicz, S. Chouaib, and B. Kaminska. 2008. Microglia-derived TGF-beta as an important regulator of glioblastoma invasion—an inhibition of TGF-beta-dependent effects by shRNA against human TGF-beta type II receptor. *Oncogene* 27: 918–930.
24. Ikushima, H., T. Todo, Y. Ino, M. Takahashi, K. Miyazawa, and K. Miyazono. 2009. Autocrine TGF-beta signaling maintains tumorigenicity of glioma-initiating cells through Sry-related HMG-box factors. *Cell Stem Cell* 5: 504–514.
25. Louis, D. N., H. Ohgaki, O. D. Wiestler, W. K. Cavenee, P. C. Burger, A. Jouvet, B. W. Scheithauer, and P. Kleihues. 2007. The 2007 WHO classification of tumours of the central nervous system. *Acta Neuropathol.* 114: 97–109.
26. DeNardo, D. G., J. B. Barreto, P. Andreu, L. Vasquez, D. Tawfik, N. Kolhatkar, and L. M. Coussens. 2009. CD4(+) T cells regulate pulmonary metastasis of mammary carcinomas by enhancing protumor properties of macrophages. *Cancer Cell* 16: 91–102.
27. Yi, L., Z. H. Zhou, Y. F. Ping, J. H. Chen, X. H. Yao, H. Feng, J. Y. Lu, J. M. Wang, and X. W. Bian. 2007. Isolation and characterization of stem cell-like precursor cells from primary human anaplastic oligoastrocytoma. *Mod. Pathol.* 20: 1061–1068.
28. Ping, Y. F., X. H. Yao, J. Y. Jiang, L. T. Zhao, S. C. Yu, T. Jiang, M. C. Lin, J. H. Chen, B. Wang, R. Zhang, et al. 2011. The chemokine CXCL12 and its receptor CXCR4 promote glioma stem cell-mediated VEGF production and tumour angiogenesis via PI3K/AKT signalling. *J. Pathol.* 224: 344–354.
29. Yi, L., H. Xiao, M. Xu, X. Ye, J. Hu, F. Li, M. Li, C. Luo, S. Yu, X. Bian, and H. Feng. 2011. Glioma-initiating cells: a predominant role in microglia/macrophages tropism to glioma. *J. Neuroimmunol.* 232: 75–82.
30. Tjiu, J. W., J. S. Chen, C. T. Shun, S. J. Lin, Y. H. Liao, C. Y. Chu, T. F. Tsai, H. C. Chiu, Y. S. Dai, H. Inoue, et al. 2009. Tumor-associated macrophage-induced invasion and angiogenesis of human basal cell carcinoma cells by cyclooxygenase-2 induction. *J. Invest. Dermatol.* 129: 1016–1025.
31. Sowinski, S., C. Jolly, O. Berninghausen, M. A. Purbhoo, A. Chauveau, K. Köhler, S. Oddos, P. Eissmann, F. M. Brodsky, C. Hopkins, et al. 2008. Membrane nanotubes physically connect T cells over long distances presenting a novel route for HIV-1 transmission. *Nat. Cell Biol.* 10: 211–219.
32. Yang, L., Y. F. Ping, X. Yu, F. Qian, Z. J. Guo, C. Qian, Y. H. Cui, and X. W. Bian. 2011. Gastric cancer stem-like cells possess higher capability of invasion and metastasis in association with a mesenchymal transition phenotype. *Cancer Lett.* 310: 46–52.
33. Mosser, D. M., and X. Zhang. 2008. Interleukin-10: new perspectives on an old cytokine. *Immunol. Rev.* 226: 205–218.
34. Kim, E. S., M. S. Kim, and A. Moon. 2004. TGF-beta-induced upregulation of MMP-2 and MMP-9 depends on p38 MAPK, but not ERK signaling in MCF10A human breast epithelial cells. *Int. J. Oncol.* 25: 1375–1382.
35. Chen, D. L., Y. F. Ping, S. C. Yu, J. H. Chen, X. H. Yao, X. F. Jiang, H. R. Zhang, Q. L. Wang, and X. W. Bian. 2009. Downregulating FPR restrains xenograft tumors by impairing the angiogenic potential and invasive capability of malignant glioma cells. *Biochem. Biophys. Res. Commun.* 381: 448–452.
36. Albini, A., and M. B. Sporn. 2007. The tumour microenvironment as a target for chemoprevention. *Nat. Rev. Cancer* 7: 139–147.
37. Lewis, C. E., and J. W. Pollard. 2006. Distinct role of macrophages in different tumor microenvironments. *Cancer Res.* 66: 605–612.
38. Murdoch, C., A. Giannoudis, and C. E. Lewis. 2004. Mechanisms regulating the recruitment of macrophages into hypoxic areas of tumors and other ischemic tissues. *Blood* 104: 2224–2234.
39. Gabrusiewicz, K., A. Ellert-Miklaszewska, M. Lipko, M. Sielska, M. Frankowska, and B. Kaminska. 2011. Characteristics of the alternative phenotype of microglia/macrophages and its modulation in experimental gliomas. *PLoS ONE* 6: e23902.
40. Wu, A., J. Wei, L. Y. Kong, Y. Wang, W. Priebe, W. Qiao, R. Sawaya, and A. B. Heimberger. 2010. Glioma cancer stem cells induce immunosuppressive macrophages/microglia. *Neuro-oncol.* 12: 1113–1125.
41. Wei, J., A. Wu, L. Y. Kong, Y. Wang, G. Fuller, I. Fokt, G. Melillo, W. Priebe, and A. B. Heimberger. 2011. Hypoxia potentiates glioma-mediated immunosuppression. *PLoS ONE* 6: e16195.
42. Psaila, B., and D. Lyden. 2009. The metastatic niche: adapting the foreign soil. *Nat. Rev. Cancer* 9: 285–293.
43. Moriyama, T., K. Ohuchida, K. Mizumoto, L. Cui, N. Ikenaga, N. Sato, and M. Tanaka. 2010. Enhanced cell migration and invasion of CD133+ pancreatic cancer cells cocultured with pancreatic stromal cells. *Cancer* 116: 3357–3368.
44. Ye, X. Z., S. C. Yu, and X. W. Bian. 2010. Contribution of myeloid-derived suppressor cells to tumor-induced immune suppression, angiogenesis, invasion and metastasis. *J. Genet. Genomics* 37: 423–430.
45. Yang, S., B. Wang, C. Guan, B. Wu, C. Cai, M. Wang, B. Zhang, T. Liu, and P. Yang. 2011. Foxp3+IL-17+ T cells promote development of cancer-initiating cells in colorectal cancer. *J. Leukoc. Biol.* 89: 85–91.
46. Cao, J. X., Y. X. Cui, Z. J. Long, Z. M. Dai, J. Y. Lin, Y. Liang, F. M. Zheng, Y. X. Zeng, and Q. Liu. 2010. Pluripotency-associated genes in human nasopharyngeal carcinoma CNE-2 cells are reactivated by a unique epigenetic submicroenvironment. *BMC Cancer* 10: 68.
47. Okuda, H., A. Kobayashi, B. Xia, M. Watabe, S. K. Pai, S. Hirota, F. Xing, W. Liu, P. R. Pandey, K. Fukuda, et al. 2012. Hyaluronan synthase HAS2 promotes tumor progression in bone by stimulating the interaction of breast cancer stem-like cells with macrophages and stromal cells. *Cancer Res.* 72: 537–547.
48. Pollard, J. W. 2008. Macrophages define the invasive microenvironment in breast cancer. *J. Leukoc. Biol.* 84: 623–630.
49. Korkaya, H., A. Paulson, F. Iovino, and M. S. Wicha. 2008. HER2 regulates the mammary stem/progenitor cell population driving tumorigenesis and invasion. *Oncogene* 27: 6120–6130.
50. Ghosh, A., M. Bhattacharya, P. Sarkar, S. Acharya, and S. Chaudhuri. 2010. T11 target structure exerts effector function by activating immune cells in CNS against glioma where cytokine modulation provide favorable microenvironment. *Indian J. Exp. Biol.* 48: 879–888.
51. Yu, S. C., Y. F. Ping, L. Yi, Z. H. Zhou, J. H. Chen, X. H. Yao, L. Gao, J. M. Wang, and X. W. Bian. 2008. Isolation and characterization of cancer stem cells from a human glioblastoma cell line U87. *Cancer Lett.* 265: 124–134.
52. Gocheva, V., H. W. Wang, B. B. Gadea, T. Shree, K. E. Hunter, A. L. Garfall, T. Berman, and J. A. Joyce. 2010. IL-4 induces cathepsin protease activity in tumor-associated macrophages to promote cancer growth and invasion. *Genes Dev.* 24: 241–255.
53. Mantovani, A., T. Schioppa, C. Porta, P. Allavena, and A. Sica. 2006. Role of tumor-associated macrophages in tumor progression and invasion. *Cancer Metastasis Rev.* 25: 315–322.
54. Coussens, L. M., C. L. Tinkle, D. Hanahan, and Z. Werb. 2000. MMP-9 supplied by bone marrow-derived cells contributes to skin carcinogenesis. *Cell* 103: 481–490.
55. Tang, Y., X. Wu, W. Lei, L. Pang, C. Wan, Z. Shi, L. Zhao, T. R. Nagy, X. Peng, J. Hu, et al. 2009. TGF-beta1-induced migration of bone mesenchymal stem cells couples bone resorption with formation. *Nat. Med.* 15: 757–765.
56. Hülper, P., W. Schulz-Schaeffer, C. Dullin, P. Hoffmann, J. Harper, L. Kurtzberg, S. Lonning, W. Kugler, M. Lakomek, and B. Erdlenbruch. 2011. Tumor localization of an anti-TGF-β antibody and its effects on gliomas. *Int. J. Oncol.* 38: 51–59.

Downloaded from http://www.jimmunol.org/ by guest on August 4, 2022